J Mater Sci (2011) 46:7877–7882
DOI 10.1007/s10853-011-5769-0

Dissipative particle dynamics simulation on the fiber dropping process of melt electrospinning

Yong Liu · Xin Wang · Hua Yan · Changfeng Guan · Weimin Yang

Received: 27 April 2011 / Accepted: 5 July 2011 / Published online: 14 July 2011

Abstract A number of theoretical problems, such as dynamic movement of molecular chains, present themselves in melt electrospinning, yet these important issues have not been thoroughly studied. In this article, a mesoscale simulation method called dissipative particle dynamics was used to study tentatively the dynamic movement of molecular chains, seeing as the diameter of spun fibers is of nanoscale dimensions, belonging to the mesoscale domain in physics. Results show that the downward traces of melting fibers are close to those obtained experimentally, the drop velocity is closely related to electrical force, the structures of the fibers differ with changes of temperature, and chain length varies at distinct descending periods.

Introduction

Increasing interest has recently been focused on electrospinning because of its potential application in the production of ultrafine fibers. Electrospinning is easier and more efficient way compared with traditional commercial fiber manufacturing methods [1–3]. In general, there are two modes by which electrospinning is performed: solution electrospinning [4, 5] and melt electrospinning [2, 6]. Most researchers employ the former because the equipment required is simpler, and it is easy to produce fibers of nanoscale dimensions. However, solution electrospinning [7, 8] presents the following major drawbacks: (1) Some solutions are expensive and extremely hazardous to the environment. (2) The production efficiency is extremely low as a result of sparse solution, and the evaporation of voluminous solvent decreases productivity. (3) It is difficult to find suitable solutions for certain polymers, such as polypropylene and polyethylene, for spinning at ambient temperatures. (4) The evaporation of solvents may cause various defects in the surface of the fibers, possibly leading to relatively low mechanical strength [9, 10].

Under elevated temperature and high electrostatic force, melt electrospinning [11] can directly produce polymer fibers, such as Zhmayev et al. [12] presented a concept of a gas-assisted polymer melt electrospinning process while McCann et al. [13] presented a technology of coaxial electrospinning. However, there have been relatively fewer studies on this field than in solution electrospinning. One possible reason is that the viscosity of a molten polymer is much higher than that in a solution; this leads to larger fiber diameters (mostly in the micron domains) as opposed to tens of nanometers when the fibers are produced in solution electrospinning. Second, the apparatus required for melt electrospinning is much more complicated than that in solution electrospinning, because a temperature control system is required to melt the polymer.

Nevertheless, a lot of research has been conducted on melt electrospinning, such as Larrondo and Manley [14], Dalton et al. [15], Deng et al. [16], and Liu et al. [17] studied the process, temperature, environment, and other factors of the method. However, few published studies have addressed theoretical problems [18], such as dynamic movement of molecular chains in the downward process and formation and distribution of supramolecular structures in fibers [19]. In an attempt to resolve the aforementioned problems, a dissipative particle dynamics (DPDs) simulation method was used, which has been adopted and adapted [20, 21] to study polymer chains [22], toroidal Structure

Y. Liu · X. Wang · H. Yan · C. Guan · W. Yang (✉)
College of Mechanical and Electrical Engineering,
Beijing University of Chemical Technology, Beijing, China
e-mail: yongsd@iccas.ac.cn

Formations [23], and melt interaction [24]. The DPD platform was built, seeing as the diameters of spun fibers are of nanoscale dimensions, belonging to the mesoscale domain in physics. All the units of DPD parameters and relative variables were reduced (i.e., dimensionless) as did usually in DPD simulations.

The models and parameters

In this study, the model system is same as those used in the previous studies [25, 26]. The simulation box, subjected to the usual periodic boundary conditions, contains 24,000 particles in 10 × 10 × 40 cubes. There are three kinds of particles in the box: those found in the surroundings or air (blue particles), polymer melt (red particles), and spinning platform (yellow particles). The air is composed of 19,200 blue particles, the melt consists of 3,353 red particles, and the spinning platform contains 1,447 yellow particles. The yellow particles are fixed and do not move along with the other particles. The red particles are connected by several springs, whereas the other particles are single, similar to the model systems described in references [27, 28]. The three kinds of particles have the same density $\rho = 6$ (each unit cube contains six particles). The parameters of conservative forces are chosen in accordance with the data in Table 1. The parameter assigned between yellow particles and the others is 80 to prevent moving particles from entering or threading into the solid spinning platform. There is no difference among the three particles in their dissipative interaction. The velocity of each particle is decided by the force endured from all the adjacent (cutoff radius is 1) particles, except for the yellow particles which are fixed. Time step is 0.02, and basic temperature is 0.10. All the initial states of melt in the model systems are the same. A polymer chain was made up of four red particles, among which the Fraenkel springs were used to express bond force [29].

The only difference between the present model systems and that in previous studies is the electrostatic forces F_{ij}^{e}, which was taken as an additional force to the conservative F_{ij}^{c}, dissipativeF_{ij}^{d}, and random forcesF_{ij}^{r}.

$$F_{ij} = F_{ij}^{c} + F_{ij}^{d} + F_{ij}^{r} + F_{ij}^{e} \quad (1)$$

Table 1 Parameters of conservative forces particles

	Red	Blue	Yellow
Red	40	30	80
Blue		12.5	80
Yellow			12.5

Unlike to the Ref. [30, 31], here the electrical force was taken as an extra body force rather an interaction between target polymer chains or different particles. The electric field exists only between the bottoms of the spinning platform and the lowest boundary of the simulation system, in which the boundary was taken as the fiber collector, as shown in Fig. 1. Here, according to experimental observation and Ref. [32], the electric field is thought not even, as shown with blue color. Herein dark blue means strong electric field, vice versa. Accordingly, the tentative electrostatic force is given by

$$F_{i} = -c(A - d_1 + d_2)\mathbf{e} \quad (2)$$

where c is a coefficient and can be used to adjust the force at will; A is a constant used to decide the basic amount of electrostatic force (15 was found to be a suitable value for the present simulation system); d_1 denotes the distance of the particle to the central axis of the simulation system, small value means big electrostatic force; d_2 represents the distance to the bottom of the spinning platform, big value means big electrostatic force; **e** is a unit vector and means the electrostatic force always points to the bottom. Usually, gravitation is weak because the spinning fiber is very thin, and the electrostatic force is the main driving force. Therefore, gravity is not considered in the present model system.

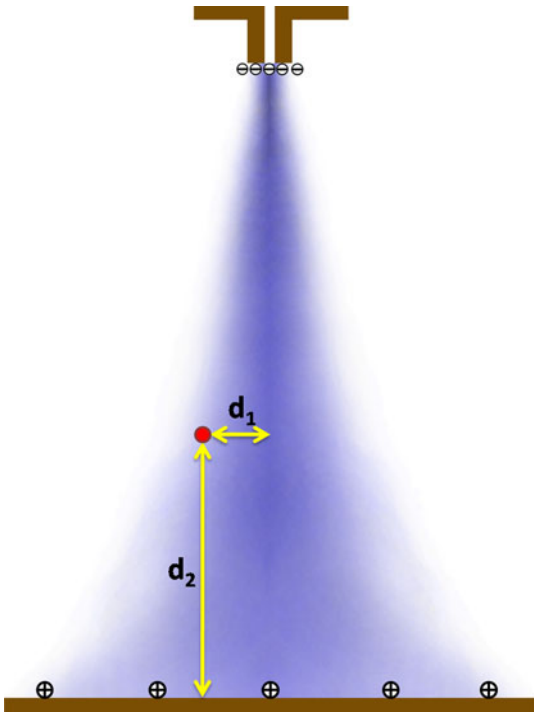

Fig. 1 Schematic of electrospinning field

Results and discussion

Simulation of dropping trace in melt electrospinning

Dropping trace is an important character of electrospinning. Researchers found that the dropping trace is more unstable in solution electrospinning especially in the field near the receiver plate, as shown in Fig. 2c) [33]. The reason for the unstable possibly contributes to the small diameter of the fiber, which is easily affected by weak disturb of air or electrostatic field. In contrast, the trace is more stable to melt electrospinning. It can be observed directly when the fiber diameter is large, as shown in Fig. 2b. Through adjusting the interactive parameter of the simulation system, the dropping trace was modeled and compared with the experimental results to justify that the new simulation system is suitable for the melt electrospinning process. As shown in Fig. 2a, the modeled dropping trace is similar to that in melt electrospinning experiment (Fig. 2b) and the pre-half trace of the solution electrospinning experiment (Fig. 2c).

Relationship between electrostatic force and dropping velocity of the fiber

Under a high electric field, both polar and non-polar polymers are polarized and produce electric charges in their inner and surface components (electric dipoles [34]). Charged polymer melt under electrostatic force is rapidly stretched, and then falls to the receiving electrode or plate. During the drop process, the polymer melt is solidified because of heat loss. Theoretically, the higher the electrostatic force, the greater polarization the polymer will undergo because the higher the charge on the melt means a higher electrostatic force was applied to it. The process of melt electrospinning and the value of electrostatic force are closely related. The relationship between voltage and fiber diameter has been investigated through experiments [17, 18], but it is difficult to measure the relationship between electrostatic force and fiber dropping rate. Therefore, a suitable simulation system was established to study the effect of electrostatic force on dropping velocity. Without changing other conditions, the electrostatic force coefficient can be modified to obtain different values of electrostatic force. Figure 3 is the morphology of fiber dropping in 3000 steps when the system temperature is 0.1 and the values of electrostatic force coefficient c are 0.65, 0.7, 0.75, 0.8, and 0.85.

As can be seen from Fig. 3, increasing electrostatic force coefficient accelerates the dropping velocity of the fiber. The average dropping velocity is calculated as shown in Fig. 4. Each set of data in this figure is an average of 10 repeated calculations because the dynamic process includes random factors. Figure 4 shows that when the coefficient of electrostatic force (which represents electrostatic force directly) increases, the dropping velocity of the fiber gradually rises. However, the change in velocity is not linear with the increase in electrostatic force. When the coefficients of electrostatic force reach a certain value, the dropping velocity rapidly increases.

Variations of temperature lead to changes in fiber structure

A higher environment temperature will extend the stretching period of fiber melt. So it is necessary to obtain

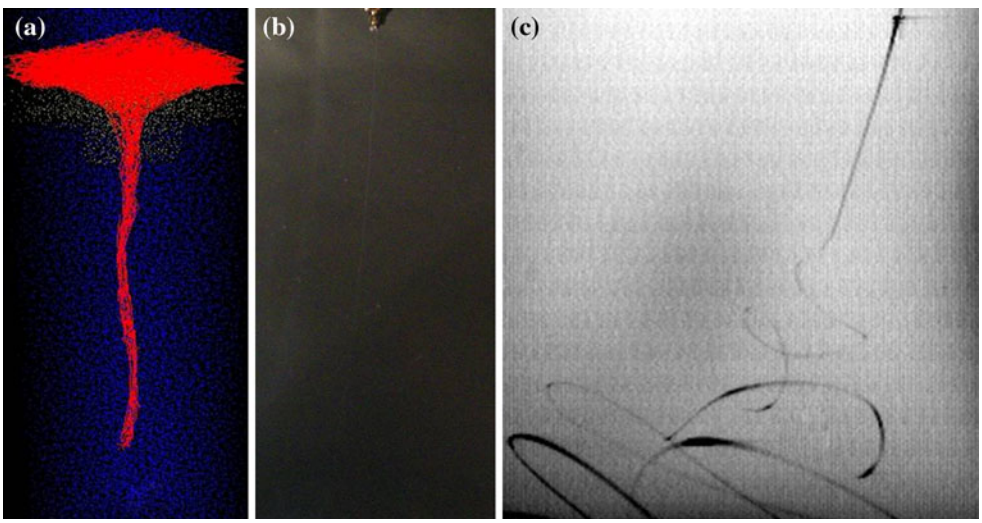

Fig. 2 Comparison of dropping traces between simulated and experimental. **a** Modeled trace; **b** snap shot of melt electrospinning trace; and **c** snap shot of solution electrospinning trace[32]

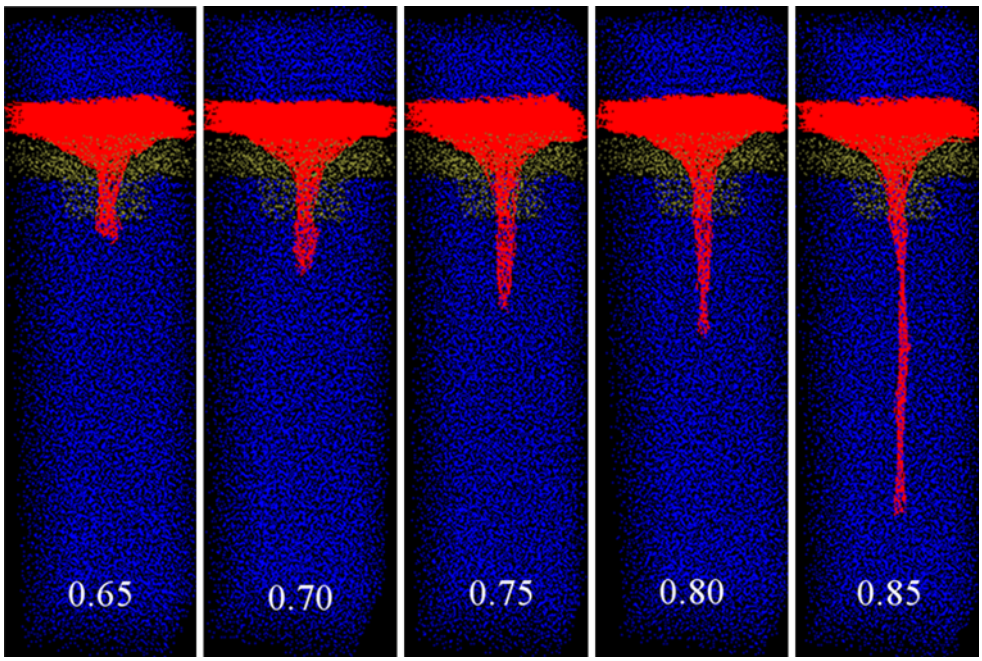

Fig. 3 Relationship between electrostatic force coefficient and dropping velocity

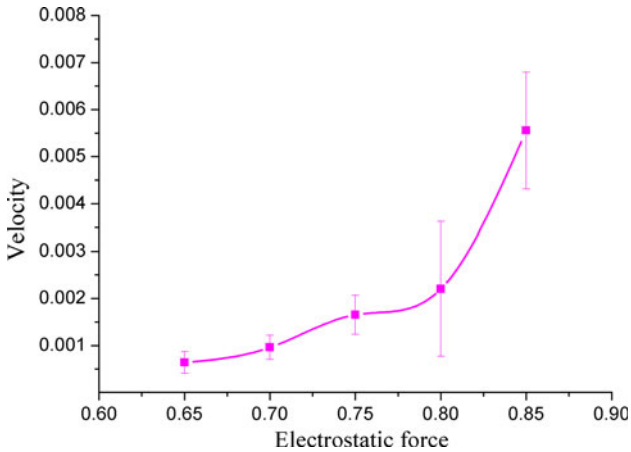

Fig. 4 Changes of dropping velocity with coefficient of electrostatic force

thinner fibers in the electrospinning experiment. However, the heat transfer between melt and air is very complicated [35, 36], and it is difficult to simulate accurately. In another side, the change of melt temperature is the key to affect the morphology of last fibers. So the present article adopted an assumption that there is no heat transfer to avoid the above problem and focused only on the melt temperature varying. The fiber dropping processes were simulated when system and fiber melt temperatures were 0.09, 0.10, 0.11, 0.12, and 0.13 using electrostatic force coefficient 0.75, and with other conditions unchanged. Results are shown in Fig. 5.

It can be seen from Fig. 5 that with the increase in temperature, the fiber gradually drops faster and its diameter becomes smaller. Particles move slowly in low temperature, and a number of molecular chains accumulate together, yielding larger fiber diameters. In experiments, when temperature was low, the melt viscosity was high, and fluidity was small. The melt flow formed quickly the thick fibers. By contrast, in a high temperature, melt can be easily stretched into thin fibers under the same electrostatic force. The abovementioned modeled results are consistent with the experimental facts [17].

Chain length during the dropping period

During melt electrospinning, the polymer melt under strong electrostatic force is stretched and its descent to the receiver plate is accelerated; thus, polymer chains are drawn continuously. Experiments cannot provide variations of molecular chains, but the length of molecular chains can be simulated. When the electrostatic force coefficient was 0.75 and temperature was 0.12, three molecular chains were selected. The end-to-end distances or chain lengths of the three chains were calculated. The change in the distances during the dropping process is shown in Fig. 6.

As shown in Fig. 6, chain lengths become longer with increasing steps, but this is not uniform throughout the entire process. Initially, the chain lengths became shorter, mainly because the chains were initially connected in the sequence of the particle ranking number, not the adjacent particles in the simulation system. Most chains will be very long because the particles were randomly dispersed in the melt area of the system at the beginning. When the system began to evolve, the excessively lengthy chains contracted or shortened. The long middle part shows that the increase in chain length is gradual. On one hand, this can be

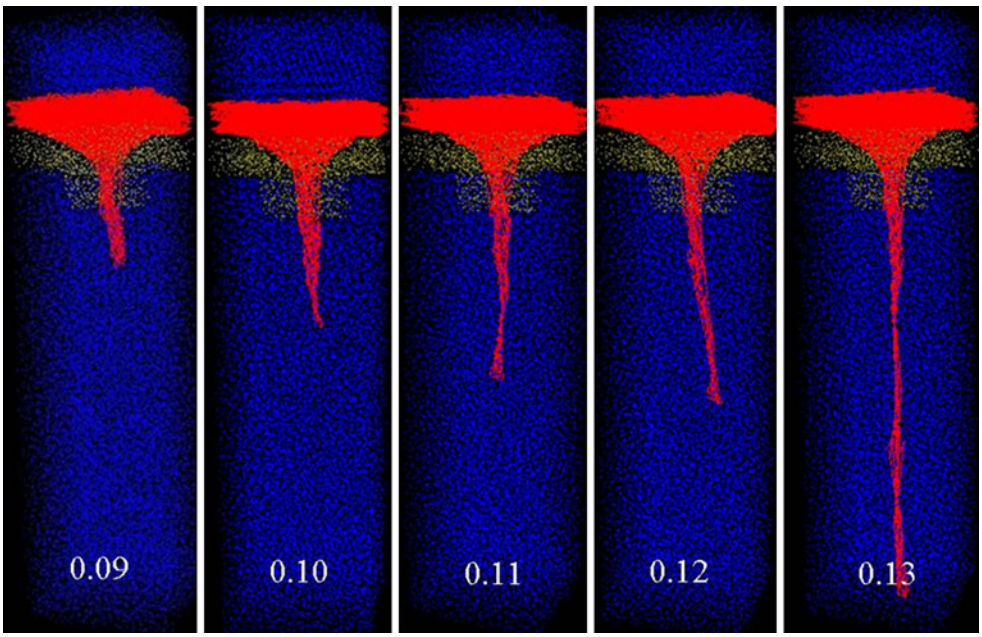

Fig. 5 Fiber dropping morphology at different temperatures

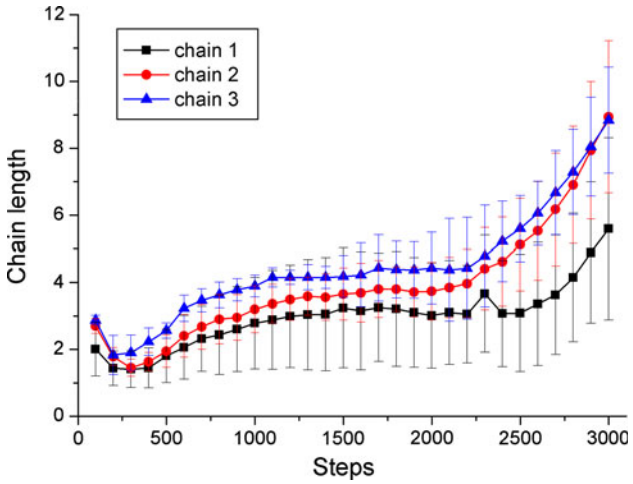

Fig. 6 Changes of chain lengths of three dropping molecules

explained by the fiber dropping velocity increasing continuously and molecular chains becoming longer at the same time. On the other hand, high dropping velocity leads to high air resistance, resulting in accelerated speed deceleration. Therefore, chain lengths increase slowly. The last part of the figure shows that the chain lengths rapidly increase, which is in accord with experiment phenomena [37] and also comply with the Fig. 4. The fast increase in chain length originates from the constantly increasing electrostatic force. The polymer is stretched extensively and chain lengths increase quickly.

Conclusion

Through trial and error, a suitable simulation system was built to model the dropping process of melt electrospinning fibers. Results show that increasing electrical field strength raises the charge density in polymers, resulting in stronger electrostatic force. Melt spinning accelerates, and so does the dropping velocity of the fiber. Increasing temperature accelerates the descent of electrospinning fibers, resulting in a dramatic decrease in fiber diameter. When fiber drops fast, chain lengths generally become longer with increasing steps. The three-period change process of chain lengths consists of shortening, gradual increase, then rapid increase in length.

Acknowledgements The authors thank Professor Ping Hu of Tsinghua University, Professor Xiaozhen Yang and Dadong Yan of the Institute of Chemistry, Chinese Academy of Science (ICCAS) for their valuable discussions.

References

1. Dzenis Y (2004) Science 304:1917
2. Hunley M, Long T (2007) Polym Int 57:385
3. Miyauchi M, Miao J, Simmons TJ, Lee JW, Doherty TV, Dordick JS, Linhardt RJ (2010) Biomacromolecules 11:2440
4. Baumgarten PK (1971) J Colloid Interface Sci 36:71
5. Hardick O, Stevens B, Bracewell DG (2011) J Mater Sci 46:3890. doi:10.1007/s10853-011-5310-5
6. Hutmacher DW, Dalton PD (2011) Chem Asian J 6:44
7. Huang ZM, Zhang YZ, Kotaki M, Ramakrishna S (2003) Compos Sci Technol 63:2223

8. Travis J, Horst AR (2008) Biomaterials 29:1989
9. Zhou FL, Gong RH, Porat I (2009) J Mater Sci 44:5501. doi: 10.1007/s10853-009-3768-1
10. Buttafoco L, Kolkman NG, Engbers-Buijtenhuijs P, Poot AA, Dijkstra PJ, Vermes I, Feijen J (2006) Biomaterials 27:724
11. Lyons J, Li C, Ko F (2004) Polymer 45:7597
12. Zhmayev E, Cho D, Joo YL (2010) Polymer 51:4140
13. McCann JT, Marquez M, Xia Y (2006) Nano Lett 6:2868
14. Larrondo L, Manley RSJ (1981) J Polym Sci Polym Phys Ed 19:909
15. Dalton PD, Grafahrend D, Klinkhammer K, Klee D, Moller M (2007) Polymer 48:6823
16. Deng RJ, Liu Y, Ding YM, Xie PC, Luo L, Yang WM (2009) J Appl Polym Sci 114:166
17. Liu Y, Deng RJ, Hao MF, Yan H, Yang WM (2010) Polym Eng Sci 50:2074
18. Zhmayev E, Cho D, Joo YL (2010) Polymer 51:274
19. Kalra V, Escobedo F, Joo YL (2010) J Chem Phys 132:024901
20. Groot RD, Warren PB (1997) J Chem Phys 107:4423
21. Espanol P (1996) Phys Rev E 53:1572
22. Symeonides V, Karmiadakis GE, Caswell B (2005) Phys Rev Lett 95:076001
23. Li XJ, Deng MG, Liu Y, Liang HJ (2008) J Phys Chem B 112:14762
24. Spaeth JR, Dale T, Kevrekidis IG, Panagiotopoulos AZ (2011) Ind Eng Chem Res 50:69
25. Liu Y, Kong B, Yang X (2005) Polymer 46:2811
26. Liu Y, Yang X, Yang M, Li T (2004) Polymer 45:6985
27. Freire JJ, Rubio AM (2008) Polymer 49:2762
28. Ibergay C, Malfreyt P, Tildesley DJ (2009) J Chem Theory Comput 5:3245
29. Liu Y, An Y, Yan H, Guan CF, Yang WM (2010) J Polym Sci B Polym Phys 48:2484
30. Groot RD (2003) J Chem Phys 118:11265
31. Gonzalez-Melchor M, Mayoral E, Velazquez ME, Alejandre J (2006) J Chem Phys 125:224107/1
32. Duan HW (2008) Design of high-voltage electrospinning machine and optimizing of electrostatic field. Ph.D. Thesis, Northeast Forestry University, China
33. http://www.nano.org.uk/news/nov2008/1688.gif. Accessed 14 June 2011
34. Service RF (2010) Science 328:304
35. Chaudhri A, Lukes JR (2009) ASME J Heat Transf 131:033108
36. Abu-Nada E (2010) Mol Simul 36:382
37. Thompson CJ, Chase GG, Yarin AL, Reneker DH (2007) Polymer 48:6913